

Supplementary Information

Binary Ni-Cu nanocomposites modified MXene adorned 3D-Nickel foam for effective overall water splitting and supercapacitor applications

Asha Raveendran^a, Mijun Chandran^b, Masoom Raza Siddiqui^c, Saikh Mohammad Wabaidur^c, Subramania Angaiah^d, Ragupathy Dhanusuraman^{a,e*}

^a*Nano Electrochemistry Lab (NEL), Department of Chemistry, National Institute of Technology Puducherry, Karaikal - 609609, India*

^b*Department of Chemistry, Central University of Tamil Nadu, Thiruvarur, 610005, India*

^c*Chemistry Department, College of Science, King Saud University, Riyadh 11451, Saudi Arabia*

^d*Electro-Materials Research Laboratory, Centre for Nanoscience and Technology, Pondicherry University, Puducherry, 605014, India*

^{a,e}*Nano Electrochemistry Laboratory (NEL), Central Instrumentation Facility (CIF), School of Physical, Chemical and Applied Sciences, Pondicherry University, Puducherry - 605014, India*

***Corresponding Author:**

Prof.Ragupathy Dhanusuraman, MRSC

Email: ragu@pondiuni.ac.in; ragu.nitpy@gmail.com

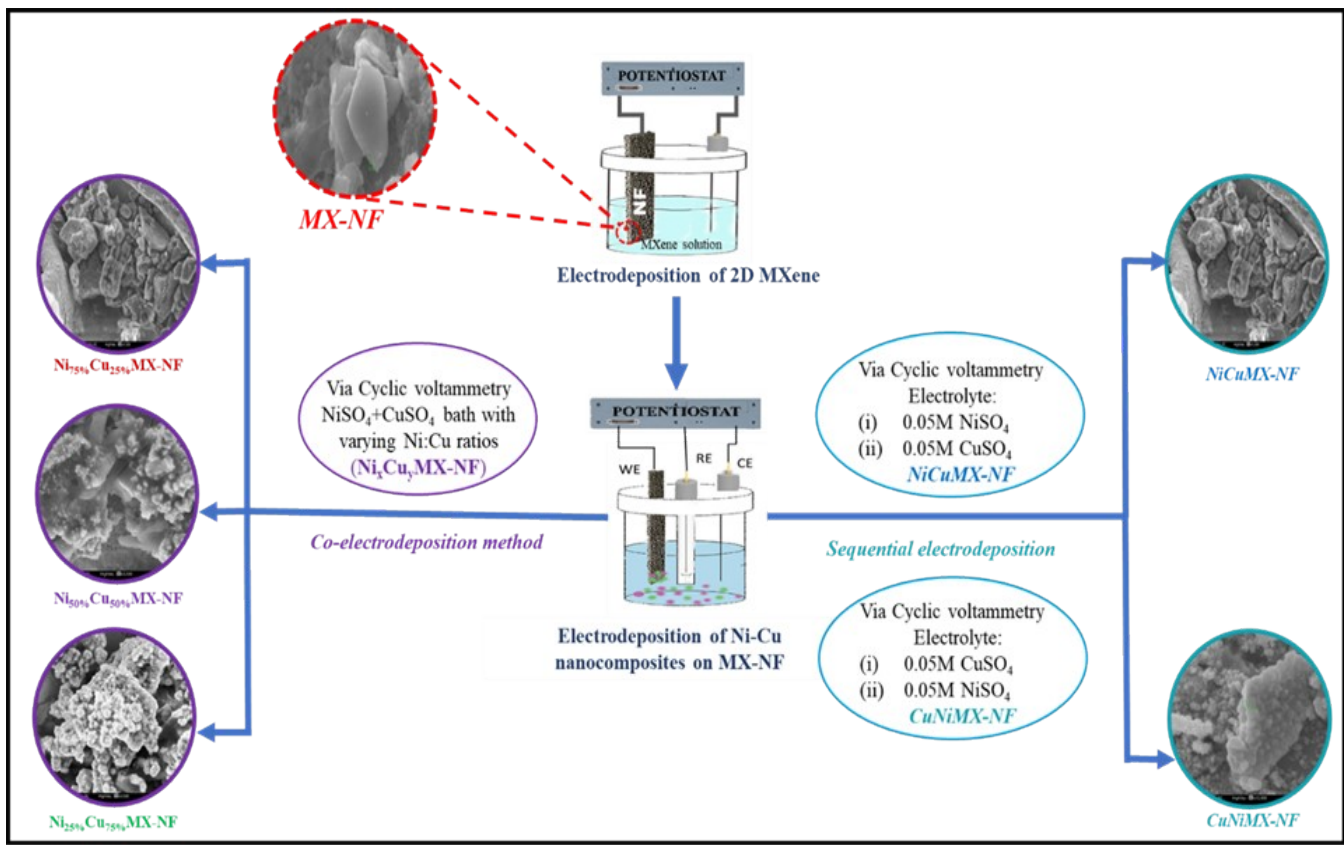


Fig S1. Schematic diagram of synthesis of electrodeposited MXene on Nickel foam followed by sequential and co-electrodeposition of bimetallic Nickel and Copper.

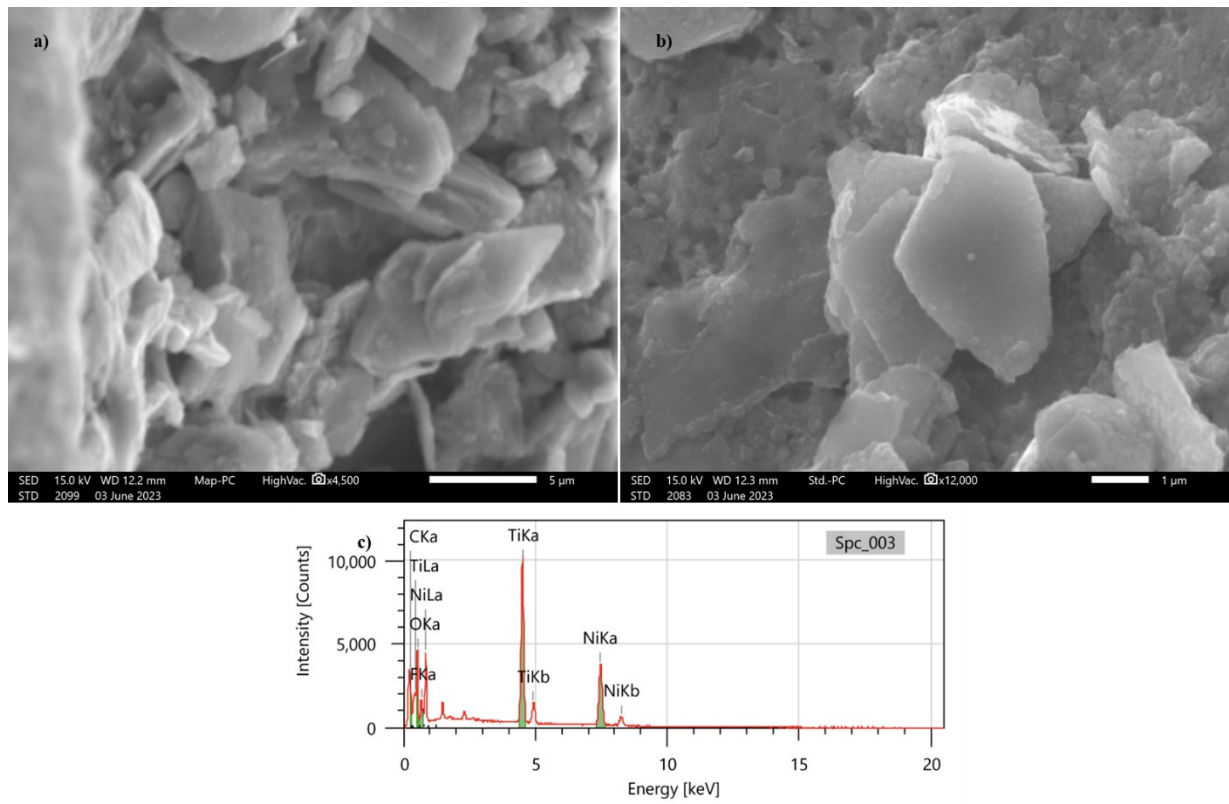


Fig. S2: (a,b) SEM images and(b) EDX spectrum of electrodeposited MXene on Nickel foam (MX-NF)

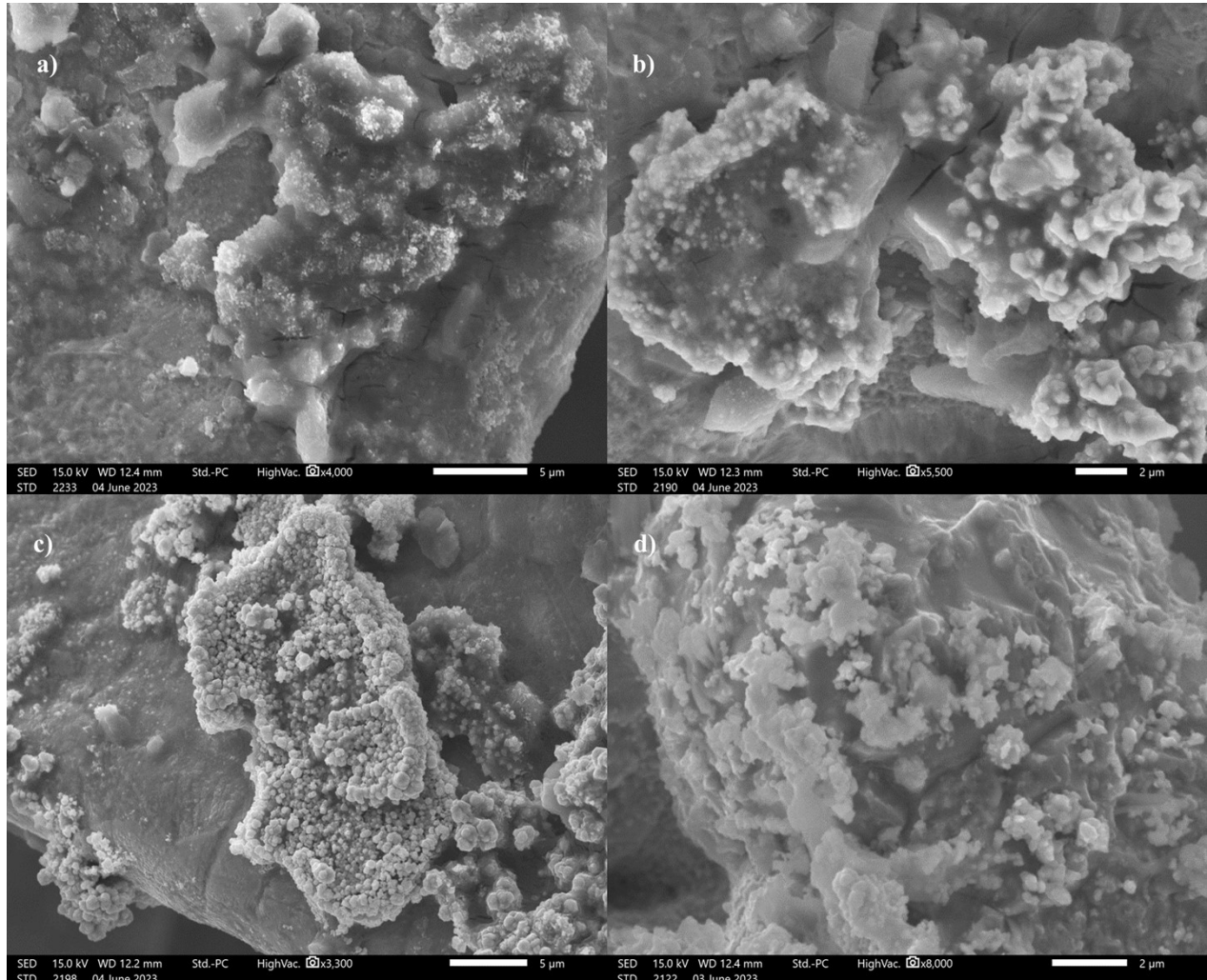


Fig. S3: SEM images of (a) Ni_{25%}Cu_{75%}MX-NF, (b) Ni_{50%}Cu_{50%}MX-NF, (c)

Ni_{75%}Cu_{25%}MX-NF and (d) CuNiMX-NF

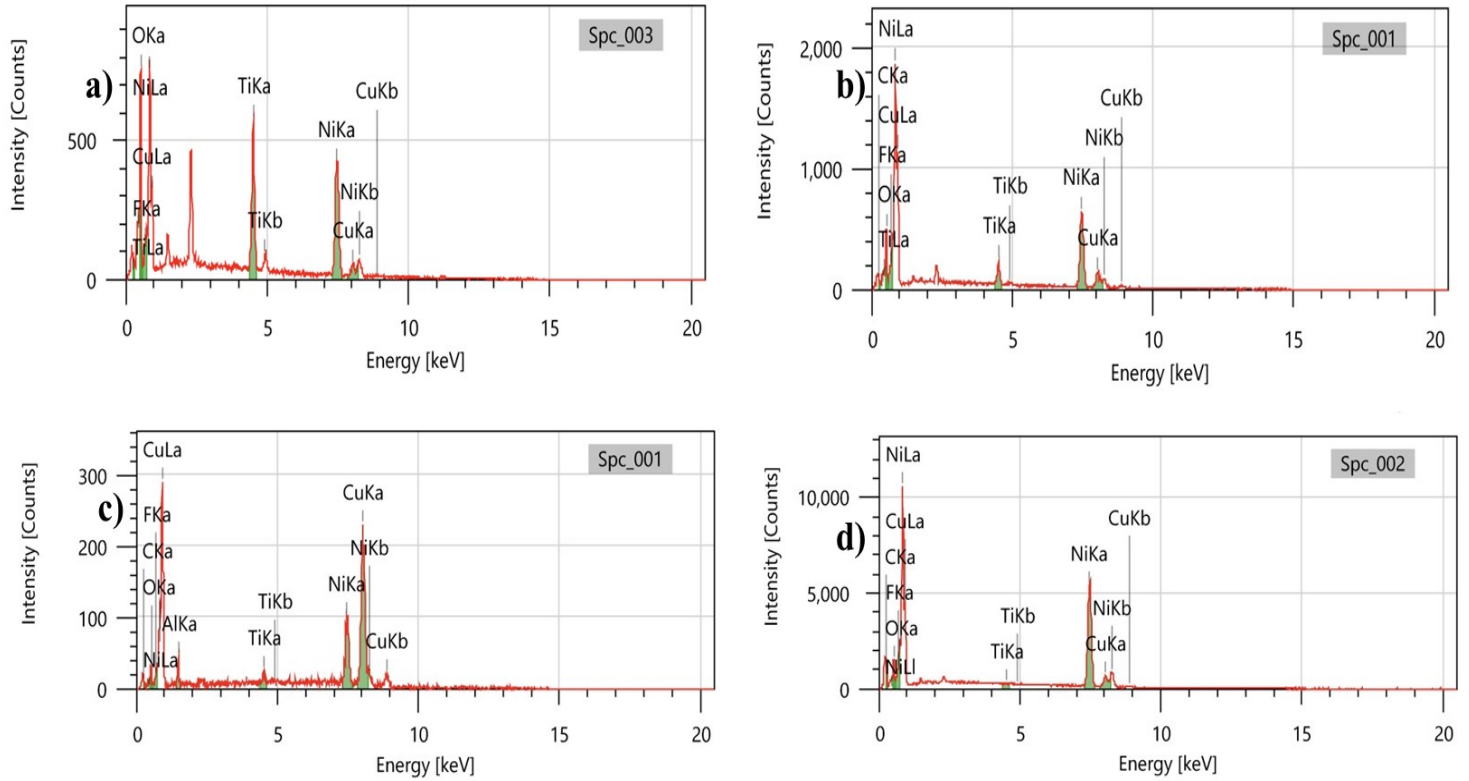


Fig. S4: EDX spectra of (a) $\text{Ni}_{25\%}\text{Cu}_{75\%}\text{MX-NF}$, (b) $\text{Ni}_{50\%}\text{Cu}_{50\%}\text{MX-NF}$, (c) $\text{Ni}_{75\%}\text{Cu}_{25\%}\text{MX-NF}$ and (d) CuNiMX-NF

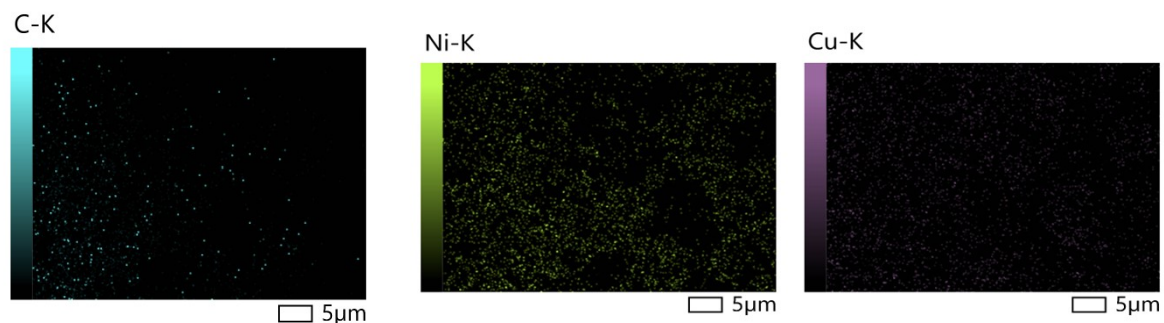
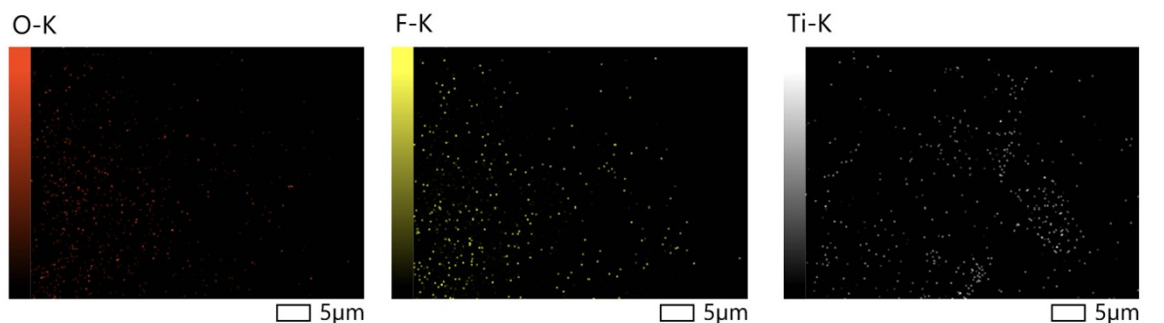
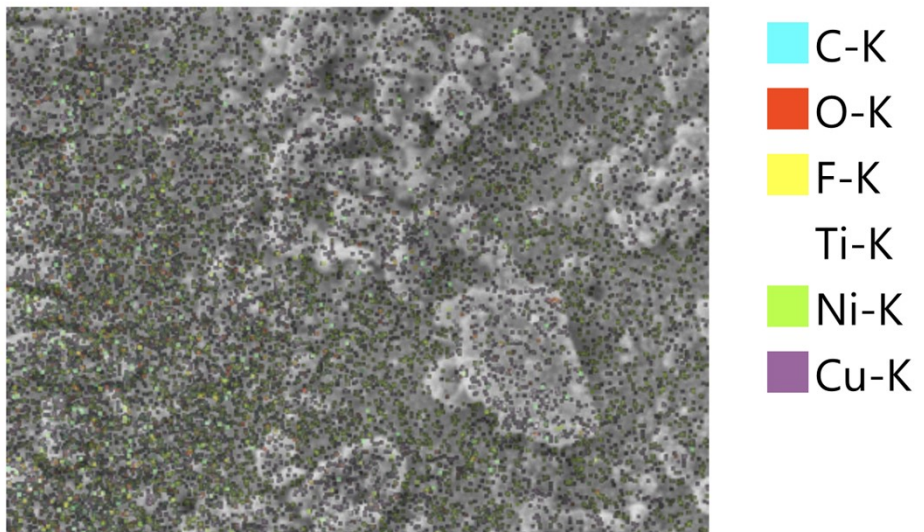


Fig. S5: (a,b) Elemental mapping of NiCuMX-NF

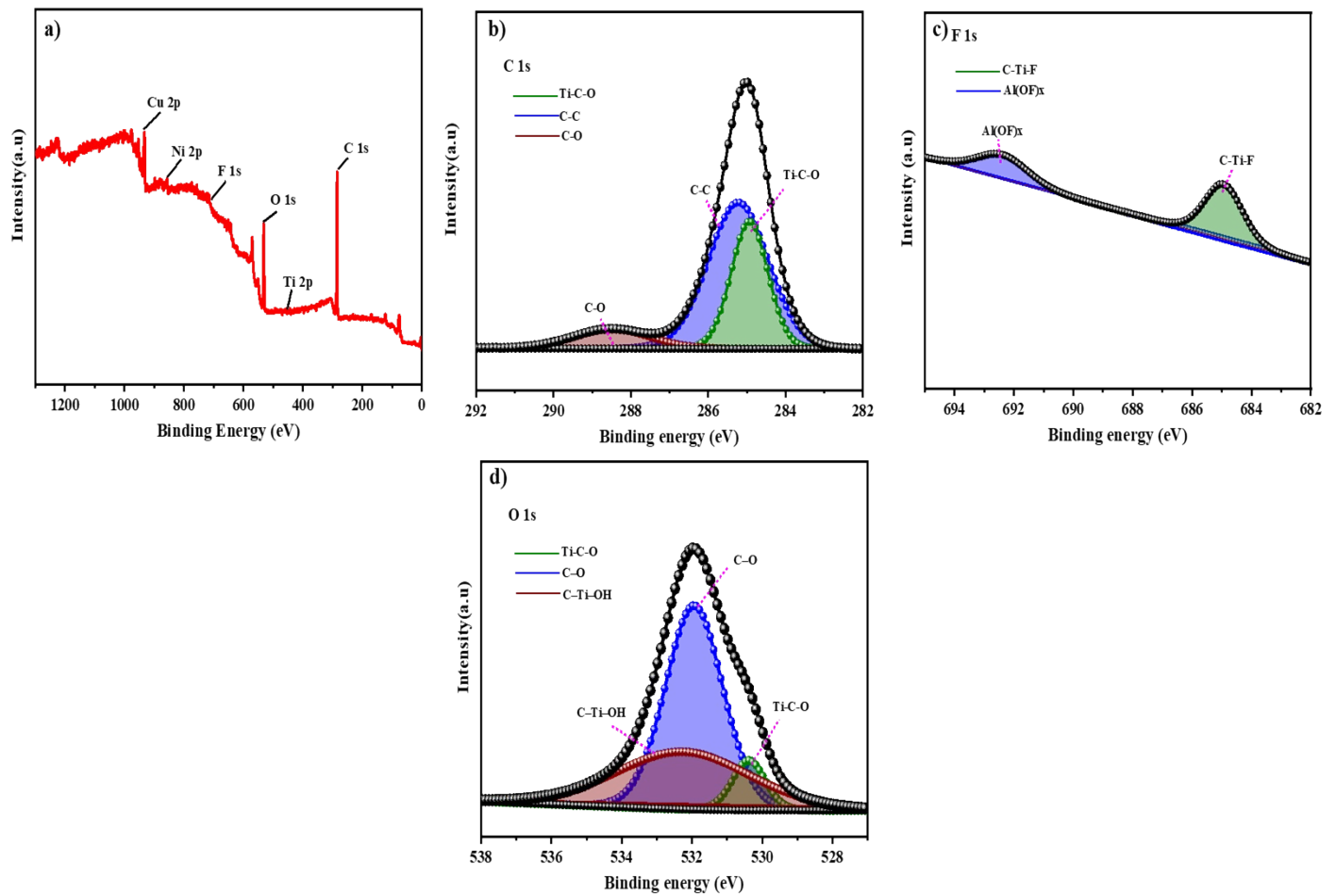


Fig. S6. X-ray photoelectron spectroscopy (XPS) spectra of (a) Overall XPS survey spectra of NiCuMX-NF and high-resolution XPS spectra of b) C 1s , (b) F 1s (c) O1s.

Calibration of reference electrodes and conversion to RHE

Using Pt wires for the working and counter electrodes and Ag/AgCl electrode as the reference electrode, a typical three-electrode setup was used to calibrate the Ag/AgCl electrode. Subsequently, 1 mV s^{-1} is applied to the linear scanning voltammetry (LSV) scan rate, and the potential at which the current crossed zero is considered the thermodynamic potential for the hydrogen electrode processes. KOH, the zero current point is at -0.273 V in 0.1M KOH hence $E(\text{RHE}) = E(\text{Ag/AgCl}) + 0.237 \text{ V}$.

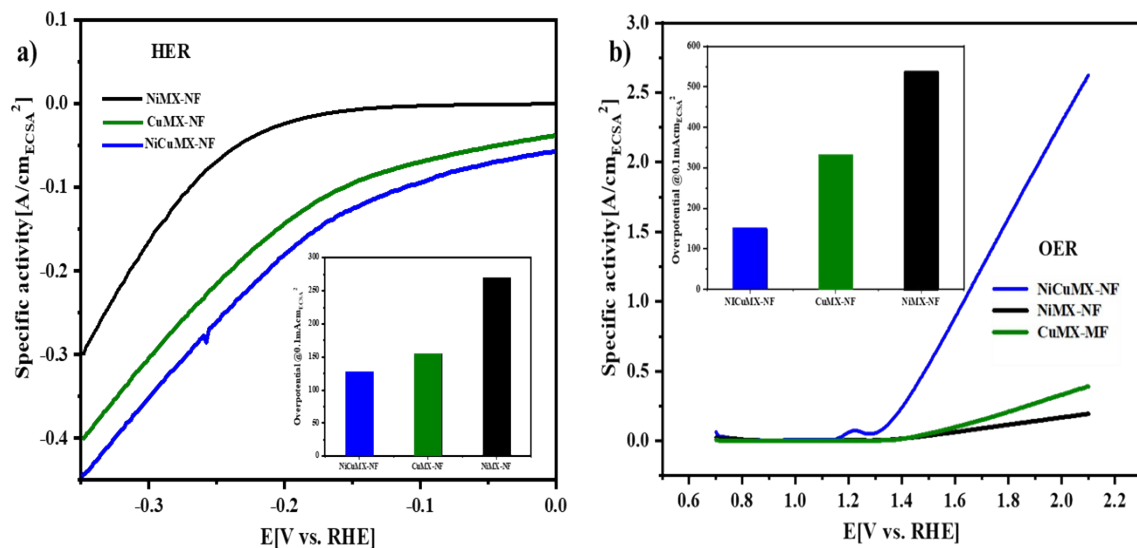


Fig. S7. Specific activity by normalizing the current with the actual electrochemical surface area (ECSA) for NiCuMX-NF, CuMX-NF and NiMX-NF (a) HER and (b) OER with their overpotentials at 0.1 mA cm^{-2} in inset

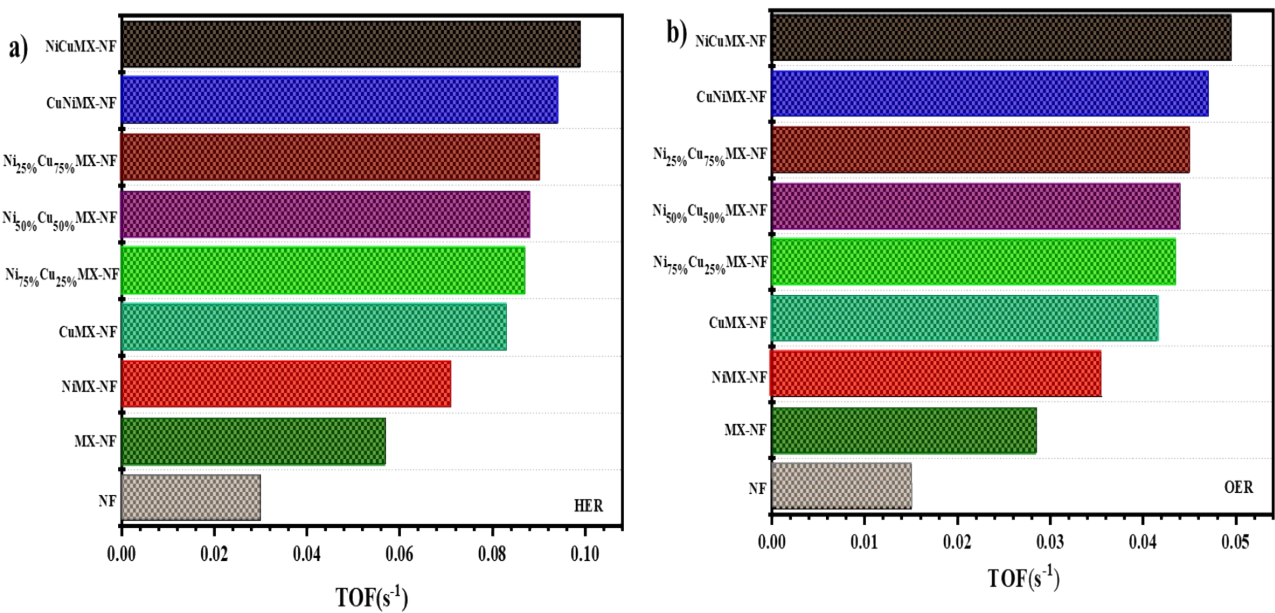


Fig. S8. TOF of the synthesised electrocatalyst at overpotential of 375mV (a) HER (b) OER

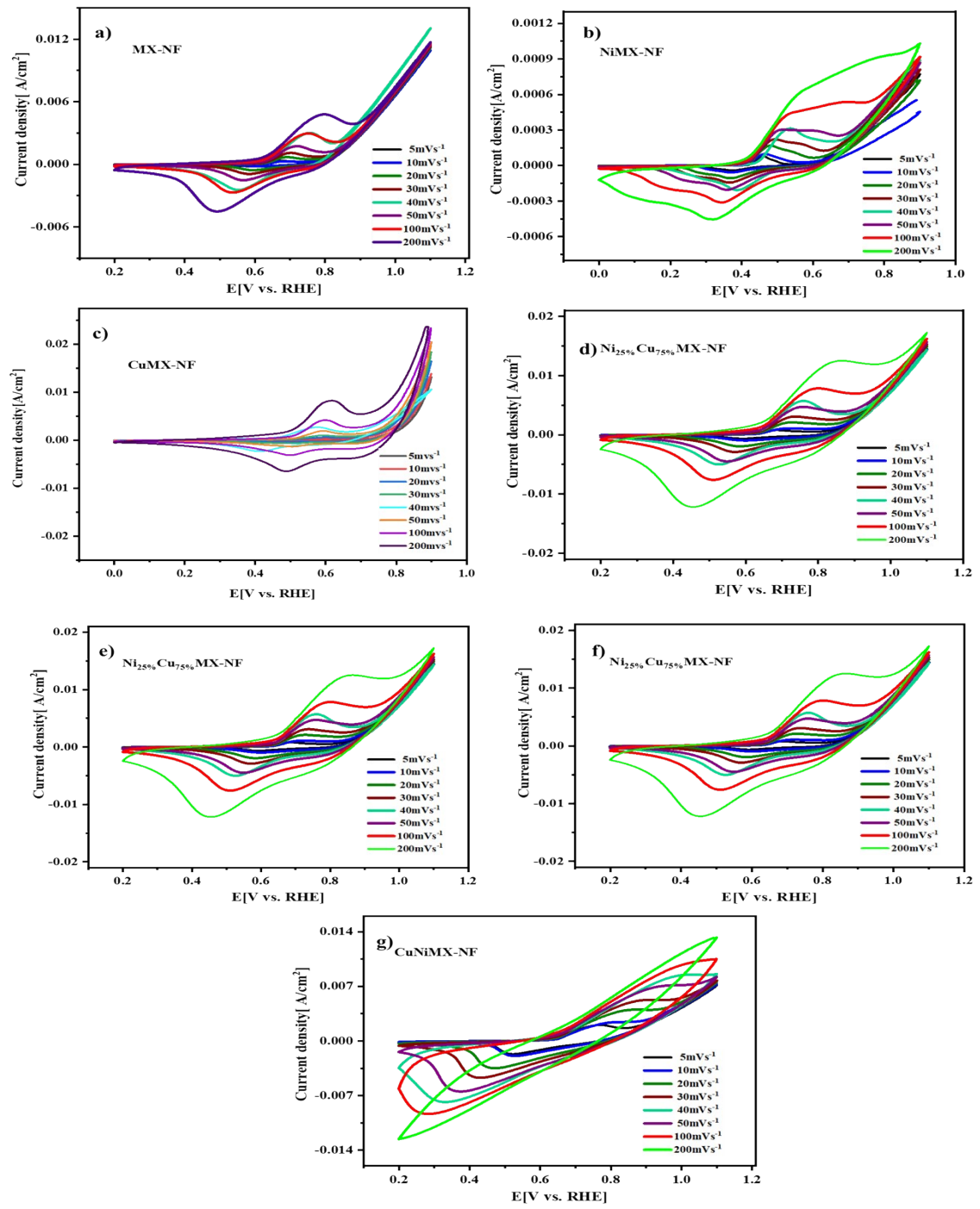


Fig. S9. Cyclic Voltammograms curves of (a) MX-NF, (b) NiMX-NF, (c) CuMX-NF, (d) $\text{Ni}_{75\%}\text{Cu}_{25\%}\text{MX-NF}$, (e) $\text{Ni}_{50\%}\text{Cu}_{50\%}\text{MX-NF}$, (f) $\text{Ni}_{25\%}\text{Cu}_{75\%}\text{MX-NF}$, (g) CuNiMX-NF at varying scan rates in 0.1M KOH

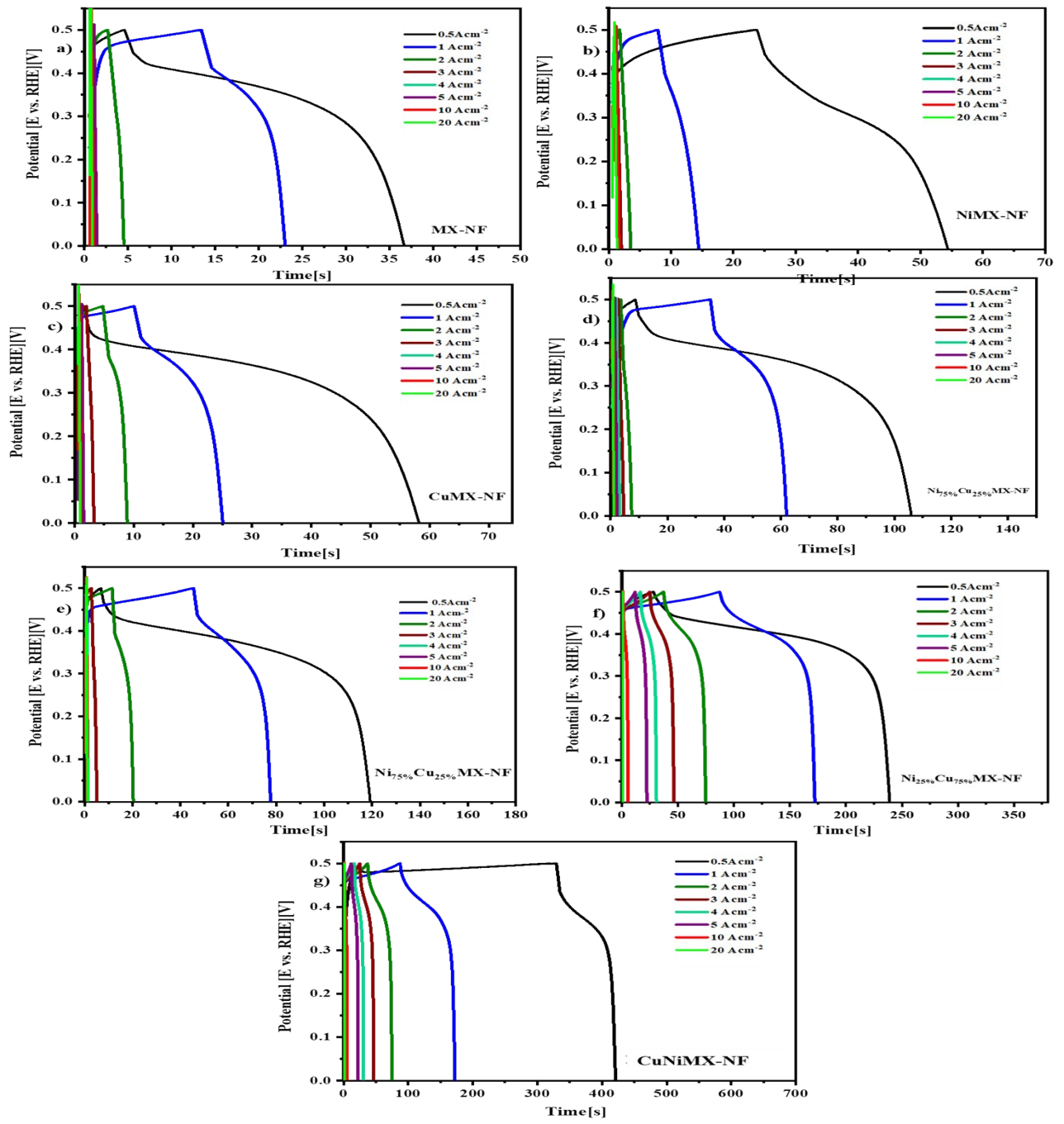


Fig. S10. Galvanostatic charge discharge curves of (a) MX-NF, (b) NiMX-NF, (c) CuMX-NF, (d) Ni_{75%}Cu_{25%}MX-NF, (e) Ni_{50%}Cu_{50%}MX-NF, (f) Ni_{25%}Cu_{75%}MX-NF, (g) CuNiMX-NF at varying current density in 0.1M KOH

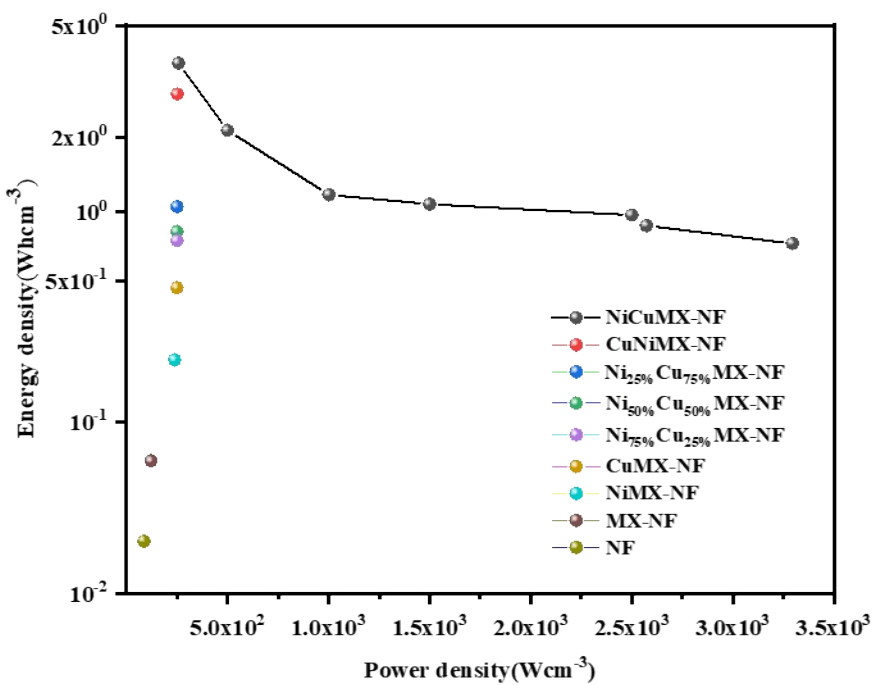


Fig. S11. Ragone plot of MX-NF, NiMX-NF, CuMX-NF, Ni_{75%}Cu_{25%}MX-NF, Ni_{50%}Cu_{50%}MX-NF, Ni_{25%}Cu_{75%}MX-NF, CuNiMX-NF and NiCuMX-NF in 0.1M KOH

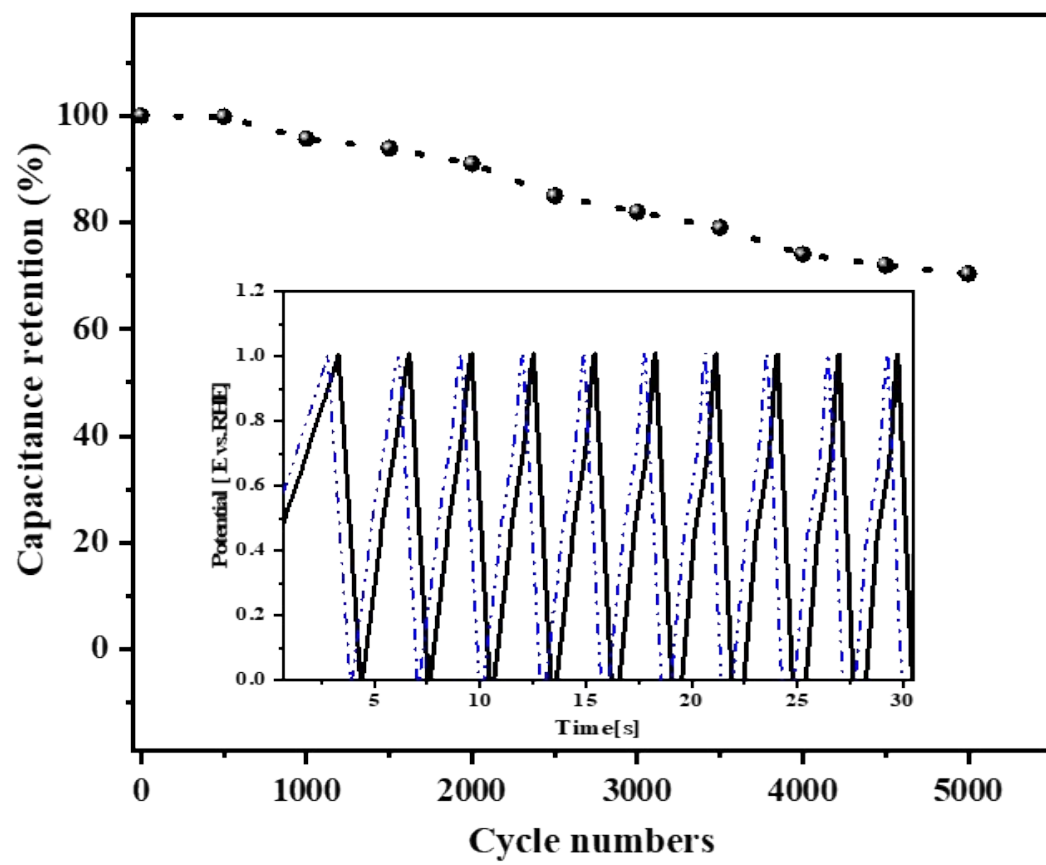


Fig S12. Capacitance retention% vs. Cycle numbers of NiCuMX-NF with inset including the comparison of cyclic stability of NiCuMX-NF for first and last ten cycles of 5000 cycles.

Table S1: A comparison of Ni_xCu_yMX-NF (2 electrode) with recently reported electrode materials

	Electrolyte	Areal Capacitance	Stability	Reference
Cu(OH) ₂ film	thin 1M NaOH	34mFcm ⁻² @ 10mVs ⁻¹	-	¹
PEDOT-Ti ₃ C ₂ T _x	PVA/1M H ₂ SO ₄	2.4mFcm ⁻² @10 mV s ⁻¹	91% after 1000 at 1A/g	²
Ti ₃ C ₂ Tx-CNF	PVA/ 1MH ₂ SO ₄	34.6mFcm ⁻² @1 mVs ⁻¹	86.8% after 10000 cycles at 10mAcm ⁻²	³
rGO-MXene	PVA/1M H ₂ SO ₄	2.4mFcm ⁻² @2 mV s ⁻¹	-	⁴
MWCNT/T _{i3} C ₂ Tx	1M H ₂ SO ₄	39mFcm ⁻² @ 1mAcm ⁻²	-	⁵
NPG-CuO	PVA-H ₂ SO ₄ electrolyte	26mFcm ⁻² @ 1 mA cm ⁻²	98% after 10000 cycles at 1 mA cm ⁻²	⁶
NiCuMX-NF	0.1M KOH	26.09mFcm ⁻² @0.5 mAcm ⁻²	70.4% after 5000 cycles at 10 mA cm ⁻²	This work

References

1. K. Gurav, U. Patil, S. Shin, G. Agawane, M. Suryawanshi, S. Pawar, P. Patil, C. Lokhande and J. Kim, *Journal of alloys and compounds*, 2013, **573**, 27-31.
2. T. Cheng, Y. W. Wu, Y. L. Chen, Y. Z. Zhang, W. Y. Lai and W. Huang, *Small*, 2019, **15**, 1901830.
3. W. Tian, A. VahidMohammadi, M. S. Reid, Z. Wang, L. Ouyang, J. Erlandsson, T. Pettersson, L. Wågberg, M. Beidaghi and M. M. Hamedi, *Advanced Materials*, 2019, **31**, 1902977.
4. C. Couly, M. Alhabeb, K. L. Van Aken, N. Kurra, L. Gomes, A. M. Navarro-Suárez, B. Anasori, H. N. Alshareef and Y. Gogotsi, *Advanced Electronic Materials*, 2018, **4**, 1700339.
5. Z. Zhou, W. Panatdasirisuk, T. S. Mathis, B. Anasori, C. Lu, X. Zhang, Z. Liao, Y. Gogotsi and S. Yang, *Nanoscale*, 2018, **10**, 6005-6013.
6. B. K. Singh, A. Shaikh, S. Badravyana, D. Mohapatra, R. O. Dusane and S. Parida, *Rsc Advances*, 2016, **6**, 100467-100475.